Real-time Calibration Algorithm for Three-axis Magnetometer

Heda Zhao[1, a], Chunsheng Lin[1, b], Hongxin Zhang[1, c]and Guojun Zhai[2]
[1]Department of Weapon Engineering, Naval University of Engineering, Wuhan 430033, China;
[2]Naval Institute of Hydrographic Surveying and Charting, Tianjin 300061, China.
[a]hd_zhao@hotmail.com,[b]lcs_and_zh@126.com,[c]mylifeforthebattle@hotmail.com

Keywords: Three - axis magnetometer, real-time calibration, state space model, Cubature Kalman Filter (CKF).

Abstract. This paper presents a real-time calibration algorithm for tri-axial magnetometer. A non-linear state space model for calibration related parameters is derived by the invariance norm of local geomagnetic field, and cubature Kalman filter (CKF) is used to estimate calibrating parameters in sequential manner, which is more suitable for real-time critical applications. The effectiveness of the algorithm are verified by numerical simulations. The results are compared with the traditional TWO-STEP algorithm, and the corresponding conclusions are obtained.

1. Introduction

The three-axis magnetometer has critical applications in attitude and heading reference system (AHRS), trajectory measurement and magnetic anomaly detection and so on. In practice, there are non-negligible errors in the output of magnetometer, which must be calibrated before being used.

The measurement errors include zero bias, non-uniform sensitivity, non-orthogonal, magnetic field offset and white noise. The maximum and minimum method[1] which calibrates the sensitivity and offset error. The TWO-STEP algorithm considering non-orthogonal factors is proposed in [2]. Similar methods based on Two-Step improves the performance using the total least squares method[3], adaptive least squares[4] and maximum likelihood estimation[5]. The abovementioned methods are all batch, which is difficult to implement in some real-time critical applications[6,7]. This paper proposed a real-time calibration algorithm for tri-axial magnetometer. A nonlinear state space model for calibration related parameters is derived according to the invariance norm of local geomagnetic field, which based a calibrating parameter estimation algorithm using cubature Kalman filter (CKF).

The structure of this paper is as follows: In section 2, the model of three-axis magnetometer is established. In section 3, the state-space model of the calibration parameters and corresponding CKF steps are derived. Numerical simulation results and analysis are given in the section 4. The section 5 summarizes the work.

2.Problem description

A three-axis magnetometer measurement model can be obtained as following,

$$\boldsymbol{B}_{r,k} = \boldsymbol{S}_M \boldsymbol{C}_{NO} (\boldsymbol{C}'_{SI} \boldsymbol{\Gamma}_{I,k}^{B} \boldsymbol{B}_k^I + \boldsymbol{b}'_{HI} + \boldsymbol{n}'_{e,k}) + \boldsymbol{b}_M + \boldsymbol{n}_{s,k} \tag{1}$$

where $\boldsymbol{S}_M$ is the scaling error diagonal matrix, $\boldsymbol{B}_{r,k}$ is the output of magnetometer at time k, $\boldsymbol{B}^I$ is local geomagnetic field. $\boldsymbol{C}_{NO}$ is the non orthogonal matrix. $\boldsymbol{C}'_{SI} = \boldsymbol{I} + \boldsymbol{C}_{SI}$, $\boldsymbol{b}'_{HI} = \boldsymbol{C}'_{SI} \boldsymbol{b}_{HI}$, $\boldsymbol{n}'_{e,k} = \boldsymbol{C}'_{SI} \boldsymbol{n}_{e,k}$. $\boldsymbol{b}_{HI}$ is the hard iron offset, $\boldsymbol{C}_{SI}$ is soft iron transform coefficient matrix, $\boldsymbol{\Gamma}_I^B$ is the rotation matrix , $\boldsymbol{b}_M$ is the zero offset, $\boldsymbol{n}_e$ is external environment noise, $\boldsymbol{n}_s$ is sensor self-noise. Eq.(1) can be further written as

$$\boldsymbol{B}_{r,k} = \boldsymbol{C}\boldsymbol{B}_K^C + \boldsymbol{b} + \boldsymbol{n}_k \tag{2}$$

where the total error matrix $\boldsymbol{C} = \boldsymbol{S}_M \boldsymbol{C}_{NO} \boldsymbol{C}'_{SI}$, total offset vector $\boldsymbol{b} = \boldsymbol{S}_M \boldsymbol{C}_{NO} \boldsymbol{b}'_{HI} + \boldsymbol{b}_M$, noise $\boldsymbol{n}_k = \boldsymbol{S}_M \boldsymbol{C}_{NO} \boldsymbol{n}'_{e,k} + \boldsymbol{n}_{s,k}$. Geomagnetic field in calibration frame $\boldsymbol{B}_k^C = \Gamma_{I,k}^B \boldsymbol{B}_k^I$. hence,

$$\boldsymbol{B}_k^C = \boldsymbol{T}(\boldsymbol{B}_{r,k} - \boldsymbol{b} - \boldsymbol{n}_k), \boldsymbol{T} = \boldsymbol{C}^{-1} \tag{3}$$

Therefore, by only estimating the matrix $\boldsymbol{T}$ and the vector $\boldsymbol{b}$, then $\boldsymbol{B}_k^C$ can be solved from the measured magnetic field $\boldsymbol{B}_{r,k}$ according to Eq. (3).

3.Real-time self-calibration algorithm

3.1 The State-Space Model of the Calibrating parameters.

Since the norm local geomagnetic field B_m is a constant, and $\boldsymbol{\Gamma}_{I,k}^B$ is orthogonal matrix, hence we have

$$\left\| \boldsymbol{B}_k^C \right\| = \left(\boldsymbol{B}_k^I \right)^T \left(\Gamma_{I,k}^B \right)^T \Gamma_{I,k}^B \boldsymbol{B}_k^I = \left\| \boldsymbol{B}_k^I \right\| = B_m^2 \tag{4}$$

Substituting Eq. (3) into (4),

$$(\boldsymbol{B}_{r,k} - \boldsymbol{b} - \boldsymbol{n}_k)^T \boldsymbol{T}^T \boldsymbol{T} (\boldsymbol{B}_{r,k} - \boldsymbol{b} - \boldsymbol{n}_k) = \boldsymbol{B}_m{}^2 \tag{5}$$

Let $\boldsymbol{T}^T \boldsymbol{T} = \boldsymbol{A}$, Eq. (5) can be written as

$$\boldsymbol{B}_{r,k}{}^T A \boldsymbol{B}_{r,k} - 2\boldsymbol{B}_{r,k}{}^T \boldsymbol{A}\boldsymbol{b} + \boldsymbol{b}^T \boldsymbol{A}\boldsymbol{b} + 2(\boldsymbol{b} - \boldsymbol{B}_{r,k})^T \boldsymbol{A}\boldsymbol{n}_k + \boldsymbol{n}_k{}^T \boldsymbol{A}\boldsymbol{n}_k = \boldsymbol{B}_m{}^2 \tag{6}$$

At this time, $\{\boldsymbol{A}, \boldsymbol{b}\}$ is the parameter to be estimated. $\boldsymbol{A}$ can be parameterized as a symmetric matrix with diagonal elements A , B , C and off-diagonal elements D , E , F . Similarly we let $\boldsymbol{b} = [b_x \ b_y \ b_z]^T$, and further we let $\boldsymbol{x} = [A \ B \ C \ D \ E \ F \ b_x \ b_y \ b_z]^T$, we have

$$\boldsymbol{x}_k = \boldsymbol{x}_{k-1} \tag{7}$$

Take the sensor output $\boldsymbol{B}_{r,k} = [B_{r,k}^x, B_{r,k}^y, B_{r,k}^z]^T$ as known parameters, the implicit measurement equation for state x can be derived directly using Eq. (6) as follows,

$$B_m{}^2 = h(\boldsymbol{x}_k) + v_k = h_1(\boldsymbol{x}_k) - 2h_2(\boldsymbol{x}_k) + h_3(\boldsymbol{x}_k) + v_k \tag{8}$$

$$h_1(\boldsymbol{x}_k) = \boldsymbol{L}_k \boldsymbol{x}_k \tag{9}$$

$$h_2(\boldsymbol{x}_k) = (AB_{r,k}{}^x + DB_{r,k}{}^y + EB_{r,k}{}^z)b_x + (DB_{r,k}{}^x + BB_{r,k}{}^y + FB_{r,k}{}^z)b_y + (EB_{r,k}{}^x + FB_{r,k}{}^y + CB_{r,k}{}^z)b_z \tag{10}$$

$$h_3(\boldsymbol{x}_k) = Ab_x{}^2 + Bb_y{}^2 + Cb_z{}^2 + 2Db_x b_y + 2Eb_x b_z 2Fb_y b_z \tag{11}$$

$$\boldsymbol{L}_k = [(B_{r,k}{}^x)^2, (B_{r,k}{}^y)^2, (B_{r,k}{}^z)^2, 2B_{r,k}{}^x B_{r,k}{}^y, 2B_{r,k}{}^x B_{r,k}{}^z, 2B_{r,k}{}^y B_{r,k}{}^z, 0, 0, 0] \tag{12}$$

$$v_k = 2(\boldsymbol{b} - \boldsymbol{B}_{r,k})^T \boldsymbol{A}\boldsymbol{n}_k + \boldsymbol{n}_k{}^T \boldsymbol{A}\boldsymbol{n}_k \tag{13}$$

where $\boldsymbol{v}_k$ is noise term. Assume $\boldsymbol{n}_k \sim \mathcal{N}(\boldsymbol{0}, \boldsymbol{N}_k)$, $\boldsymbol{N}_k = E[\boldsymbol{n}_k \boldsymbol{n}_k{}^T]$ is the noise covariance matrix.

To sum up, the calibrating parameter state space model can be obtained as follows

$$\begin{aligned} \boldsymbol{x}_k &= \boldsymbol{x}_{k-1} \\ \boldsymbol{y}_k &= h(\boldsymbol{x}_k) + v_k \end{aligned} \tag{14}$$

$y_k = B_m{}^2, k = 1, 2, ..., N$, N is the number of samples measured. Through Eq. (8)-(14), we convert the real-time self-calibration problem into the filter estimation of the calibrating parameters.

3.2 Cubature Kalman Filter (CKF).

CKF is a LMMSE filter based on the third-order cubature rule. $\hat{\boldsymbol{x}}_{k-1}$ is the state estimation value at time $k-1$; $\boldsymbol{P}_{k-1}$ is the state covariance matrix at time $k-1$. Since the state is constant, hence the time update is simply

$$\hat{\boldsymbol{x}}_k^- = \hat{\boldsymbol{x}}_k \, , \boldsymbol{P}_k^- = \boldsymbol{P}_{k-1} \tag{15}$$

For the measurement update, we first calculate the cubature points as,

$$\boldsymbol{X}_{i,k} = \sqrt{\boldsymbol{P}_k^-} \xi_i + \hat{\boldsymbol{x}}_k^-, \boldsymbol{Z}_{i,k} = h(\boldsymbol{X}_{i,k}), i = 1, 2, \cdots, 2n \tag{16}$$

further we calculate the prediction $\hat{\boldsymbol{z}}_k^-$, the innovation covariance $\boldsymbol{P}_{zz,k}$ and the cross covariance $\boldsymbol{P}_{xz,k}$, We finally get measurement updates as

$$\boldsymbol{P}_{zz,k} = \frac{1}{2n}\sum_{i=1}^{2n}\boldsymbol{Z}_{i,k}\boldsymbol{Z}_{i,k}^{T} - \hat{\boldsymbol{z}}_k^{-}\hat{\boldsymbol{z}}_k^{-T} + r_k,\ \boldsymbol{P}_{xz,k} = \frac{1}{2n}\sum_{i=1}^{2n}\boldsymbol{X}_{i,k}\boldsymbol{Z}_{i,k}^{T} - \hat{\boldsymbol{x}}_k^{-}\hat{\boldsymbol{z}}_k^{-T} \tag{17}$$

$$\hat{\boldsymbol{x}}_k = \hat{\boldsymbol{x}}_k^{-} + \boldsymbol{K}_k(z_k - \hat{\boldsymbol{z}}_k^{-}) \tag{18}$$

where $\hat{\boldsymbol{z}}_k^{-} = 1/2n\sum_{i=1}^{2n}\boldsymbol{Z}_{i,k}$, $\boldsymbol{K}_k = \boldsymbol{P}_{xz,k}\boldsymbol{P}_{zz,k}^{-1}$, $\boldsymbol{P}_k = \boldsymbol{P}_k^{-} - \boldsymbol{K}_K\boldsymbol{P}_{zz,k}\boldsymbol{K}_k^{T}$, $r_k = E[v_k v_k{}^{T}]$.

Since $\boldsymbol{A} = \boldsymbol{T}^{T}\boldsymbol{T}$ is a symmetric matrix. The singular value decomposition [4] of $\boldsymbol{A}$ is performed as

$$\boldsymbol{A} = \boldsymbol{Q}\Sigma\boldsymbol{Q}^{T} \tag{19}$$

where Σ is a diagonal matrix, we thus have

$$\boldsymbol{T} = \boldsymbol{Q}\sqrt{\Sigma}\boldsymbol{Q}^{T} \tag{20}$$

By the calibration parameters $\boldsymbol{T},\boldsymbol{b}$, the calibrated magnetometer output can be obtained by Eq. (3).

4.Results and Analysis

In this section, the proposed method is verified by the simulation data. The results of the two-step calibration algorithm are also given as comparison. More detailed about TWO-STEP calibration method can be found in [1]. The non-orthogonal error angles are $\rho = 2°$, $\phi = 1°$, $\lambda = 1.5°$ .The scaling $\boldsymbol{S}_M = diag(1.2, 0.8, 1.3)$, hard iron $\boldsymbol{b}_{HI} = [-1.2, 0.2, -0.8]^T$ G , the zero bias $\boldsymbol{b}_M = [1.5, 0.4, 2.7]^T$ G , and the soft iron matrix are with elements less than 0.25 .The local geomagnetic field at the measuring point is $\boldsymbol{B}^I = [0.33, 0.024, 0.36]^T$ G in the NED frame. The noise density is $\boldsymbol{N}_k = \mathrm{diag}(\sigma^2, \sigma^2, \sigma^2)$, $\sigma = 0.05$G . The random attitude quaternion $\boldsymbol{q} = [\cos(0.5\theta), \sin(0.5\theta)\boldsymbol{u}^T]^T$ is used to simulate the rotation operation.

Table 1 Results of the parameter estimation

	$\boldsymbol{A}$	$\boldsymbol{b}$
Ground true	$\begin{bmatrix} 0.824 & 0.261 & -0.359 \\ 0.261 & 1.084 & -0.202 \\ -0.359 & -0.202 & 0.554 \end{bmatrix}$	$\begin{bmatrix} -0.331 \\ 0.632 \\ 1.006 \end{bmatrix}$
Proposed method	$\begin{bmatrix} 0.816 & 0.247 & -0.354 \\ 0.247 & 1.068 & -0.192 \\ -0.354 & -0.192 & 0.556 \end{bmatrix}$	$\begin{bmatrix} -0.328 \\ 0.633 \\ 1.010 \end{bmatrix}$
TWO-STEP	$\begin{bmatrix} 0.817 & 0.255 & -0.367 \\ 0.255 & 1.057 & -0.204 \\ -0.367 & -0.204 & 0.569 \end{bmatrix}$	$\begin{bmatrix} -0.332 \\ 0.631 \\ 1.007 \end{bmatrix}$

Table 1 shows the average results of parameter estimation using the proposed method and the Two-Step method after 50 Monte Carlo simulations. Obviously the real-time algorithm can estimate the parameters with good accuracy and the result is in the neighborhood with Two-Step method. Figure 1 shows the total field norm before and after calibration. It is shown that the norm of raw data are fluctuated significantly in the range of 0.6~2Gauss, while the norm after calibration are stable in the range of about 0.1 Gauss around the reference geomagnetic field. And close to the result after the TWO-STEP calibration. Figure 2 shows the measured geomagnetic field in the sensor frame before and after the calibration. The readings before calibration is distributed as ellipsoid, and the calibrated readings is a sphere with reference geomagnetic norm as its radius.

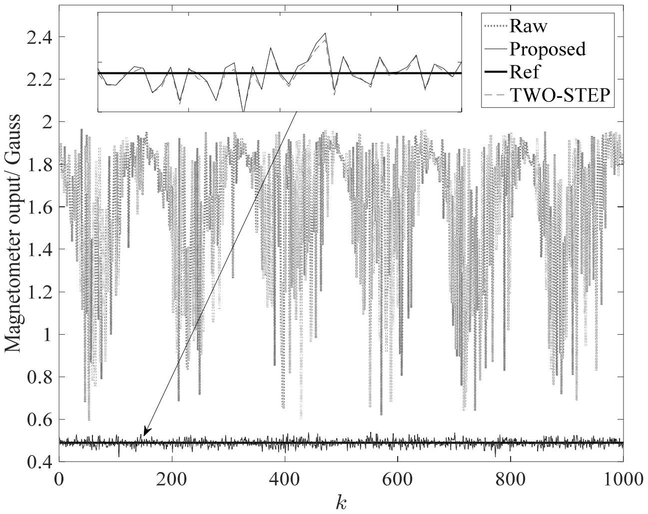

Fig.1 local geomagnetic field norm: Before and after calibration

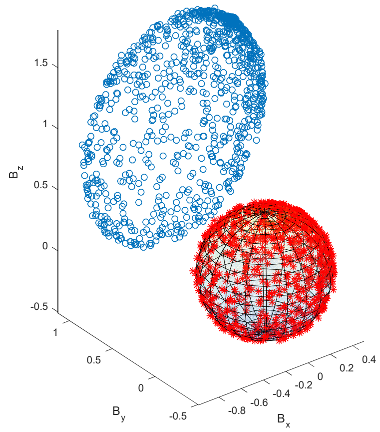

Fig.2 Sensor frame readings: Before and after calibration

5.Summary

A real-time calibration algorithm of tri-axial magnetometer is proposed. The proposed method overcomes the shortcomings of the off-line algorithm. Compared with the offline algorithm, this algorithm is more suitable for high real-time platform and which is difficult to implement a second calibration.

Acknowledgments

This work was supported by National Science Foundation (41374018, 41476087) and the National Research and Development Fund for Scientific Research Equipment (ZDYZ2012-1).

References

[1] Foster C C, Elkaim G H. Extension of a two-step calibration methodology to include non-orthogonal sensor axes[J]. Aerospace & Electronic Systems IEEE Transactions on, 2008, 44(3):1070-1078.

[2] Peng X D, Zhang T M, Li J Y. Attitude estimation algorithm of agricultural small-UAV based on sensors fusion and calibration[J]. Acta Automatica Sinica, 2015, 41(4):854-860.

[3] Wu Z, Hu X, Wu M, et al. Attitude-independent magnetometer calibration for marine magnetic surveys: regularization issue[J]. Journal of Geophysics & Engineering, 2013, 10(4):45002-45010(9).

[4] Valérie R, Afzal M H, Gérard L. Complete Triaxis Magnetometer Calibration in the Magnetic Domain[J]. Journal of Sensors, 2010, 2010(1):23-59.

[5] Vasconcelos F, Elkaim G, Silvestre C, et al. Geometric Approach to Strapdown Magnetometer Calibration in Sensor Frame[J]. IEEE Transactions on Aerospace &Electronic Systems, 2011, 47(2):1293-1306.

[6] Grandvallet B, Zemouche A, Boutayeb M, et al. Real-Time Attitude-Independent Three-Axis Magnetometer Calibration for Spinning Projectiles: A Sliding Window Approach[J]. IEEE Transactions on Control Systems Technology, 2014, 22(1):255-264.

[7] Crassidis J L, Lai K L, Harman R R. Real-Time Attitude-Independent Three-Axis Magnetometer Calibration[J]. Journal of Guidance Control & Dynamics, 2005, 28(1): 115-120